

All-fabric-based wearable self-charging power cloth

Yu Song, , Jinxin Zhang, , Hang Guo, , Xuexian Chen, , Zongming Su, , Haotian Chen, , Xiaoliang Cheng, and ,
and Haixia Zhang

Citation: *Appl. Phys. Lett.* **111**, 073901 (2017); doi: 10.1063/1.4998426

View online: <http://dx.doi.org/10.1063/1.4998426>

View Table of Contents: <http://aip.scitation.org/toc/apl/111/7>

Published by the [American Institute of Physics](#)



CiSE magazine is
an innovative blend.

COMPUTING

ENGINEERING

SCIENCE

Computing
in SCIENCE & ENGINEERING

EXPLORING OUR
SOLAR SYSTEM

All-fabric-based wearable self-charging power cloth

Yu Song,¹ Jinxin Zhang,¹ Hang Guo,^{1,2} Xuexian Chen,^{1,2} Zongming Su,¹ Haotian Chen,^{1,2} Xiaoliang Cheng,¹ and Haixia Zhang^{1,2,a)}

¹National Key Lab of Nano/Micro Fabrication Technology, Institute of Microelectronics, Peking University, Beijing 100871, China

²Academy for Advanced Interdisciplinary Studies, Peking University, Beijing 100871, China

(Received 22 May 2017; accepted 25 June 2017; published online 14 August 2017)

We present an all-fabric-based self-charging power cloth (SCPC), which integrates a fabric-based single-electrode triboelectric generator (STEG) and a flexible supercapacitor. To effectively scavenge mechanical energy from the human motion, the STEG could be directly woven among the cloth, exhibiting excellent output capability. Meanwhile, taking advantage of fabric structures with a large surface-area and carbon nanotubes with high conductivity, the wearable supercapacitor exhibits high areal capacitance (16.76 mF/cm^2) and stable cycling performance. With the fabric configuration and the aim of simultaneously collecting body motion energy by STEG and storing in supercapacitors, such SCPC could be easily integrated with textiles and charged to nearly 100 mV during the running motion within 6 min, showing great potential in self-powered wearable electronics and smart cloths. *Published by AIP Publishing.* [<http://dx.doi.org/10.1063/1.4998426>]

Personal electronics attract great attention when the pursuit of multi-functionality and intelligence has inevitably become a significant trend.^{1,2} This advancement requires not only miniaturization of various electronic components but also the integration with cloths and accessories.³ Lightweight and wearable power supply modules with high performance are desirable for the progress of smart electronics.⁴ Therefore, wearable self-charging power systems that integrate the energy-harvesting and energy-storing technologies could be the potential solution.⁵⁻⁷

On the one hand, considering the fact that energy storage devices, such as batteries and supercapacitors,⁸⁻¹⁰ face inconvenient charging by the external supply, researchers have proposed self-charging electronics by integration of flexible supercapacitors with solar cells.¹¹ However, a photovoltaic cell is not always available and strongly dependent on the weather and working conditions. The intermittent and unpredictable characteristic of solar energy seems great challenge for the reliable power supply in wearable electronics.

On the other hand, with the development of energy harvesters, such as triboelectric nanogenerators,¹²⁻¹⁴ they have been widely studied to scavenge different mechanical energies without the restriction of environments. By using triboelectric nanogenerators as the power supply, various types of self-powered systems are demonstrated.¹⁵⁻¹⁷ However, most of them are applied with the contact-separation mode,^{18,19} which requires large space and limits its application in cloth integration.

Herein, we present a prototype of an all-fabric-based self-charging power cloth (SCPC) by integrating a wearable single-electrode triboelectric generator (STEG) and a flexible supercapacitor with a general carbon nanotube (CNT)/cotton fabric electrode. Woven among the body side cloth, STEG could scavenge the human mechanical energy effectively, which could be simultaneously converted into

electrochemical energy and stored in the supercapacitor. Our proposed SCPC not only achieves reliable energy harvesting efficiency and storage capacity but also demonstrates high integration and working compatibility, thus demonstrating promising candidates for operating wearable devices.

The fabric-based structure of our proposed SCPC is schematically illustrated in Fig. 1(a) that combines two functional units: STEG for the energy harvesting and the flexible supercapacitor for energy storage. To meet the demands of the integrated SCPC, a general cotton fabric electrode is

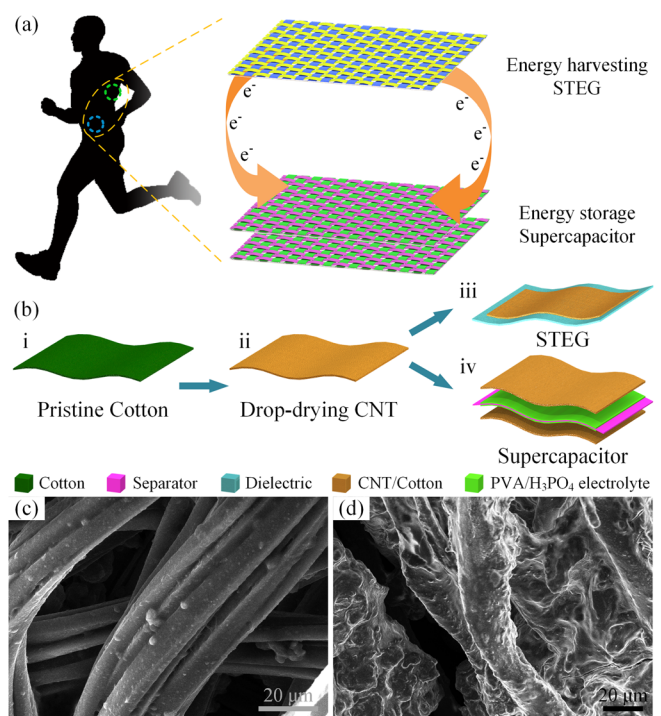


FIG. 1. (a) Schematic of the all-fabric-based self-charging power cloth, which is made of a wearable STEG and a flexible supercapacitor. (b) Fabrication process of SCPC with a general CNT/cotton fabric electrode. SEM images of (c) pristine and (d) CNT coated cotton fabric.

^{a)}Electronic mail: zhang-alice@pku.edu.cn

developed due to its remarkable flexibility, porosity, and compatibility.²⁰ In addition, multiwalled CNT is selected to compound with the cotton fabric with high conductivity and strong chemical attachment with the cotton fiber. After the SCPC is attached among the cloth, the body motion energy could be scavenged by the STEG and stored in the supercapacitors.

The detailed fabrication of SCPC is shown in Fig. 1(b). The general CNT/cotton fabric electrodes are simply fabricated by using the drop-drying method. First, the commercially flexible cotton fabric (20 cm²) is cleaned with ethanol and deionized water. Then, the CNT ink solution is prepared by dispersing CNTs (100 mg) and 100 mg sodium dodecylbenzenesulfonate (SDBS) as a surfactant in 100 ml of deionized water and bath-sonicated for 4 h to disperse evenly. The cotton fabric is dropped by the CNT ink solution and dried at 90 °C several times until the CNTs are saturated as the active materials. On the one hand, the wearable STEG is prepared after the CNT/cotton fabric electrode is attached to the dielectric layer, such as nylon, cotton, or other fabric clothes. On the other hand, for the flexible supercapacitor, 6 g phosphoric acid (H₃PO₄) is mixed with 60 ml deionized water and 6 g polyvinyl alcohol (PVA) powder. The mixture is heated up to 85 °C under vigorous stirring until the solution becomes clear. Coated with the PVA/H₃PO₄ gel electrolyte, a cellulose separator is assembled with two pieces of CNT/cotton fabric electrodes. Subsequently, the prepared solid-state supercapacitor is left in the fume hood at room temperature to fully vaporize the excess water. Integrated with the STEG, the whole SCPC is finally developed.

With the proposed process, the general CNT/cotton fabric electrode has been fabricated. Scanning electron microscopy (SEM) images in Figs. 1(c) and 1(d) clearly demonstrate the morphologies of pristine and CNT coated cotton fabric, respectively. It could be observed that CNTs are densely coated on the surfaces of fibers and form the conductive network. This conductive fabric exhibits excellent flexibility as shown in Fig. S1, which meets the requirement of wearable devices. In addition, Fig. S2 presents the change in resistance, where the resistance decreases significantly with the increasing dropping times. Considering the fact that the washing stability of the conductive fabric is crucial to the wearable electronics, the resistance of the prepared CNT/cotton fabric with washing time is evaluated as shown in Fig. S3. Obviously, such conductive fabric shows good durability after being rinsed with deionized water and bath-sonicated several times, which could be utilized as wearable electrical textile.

The working mechanism of the SCPC is described in Fig. 2, where the device works based on the coupling effects of contact electrification and electrostatic induction. To meet the demands of SCPC, we choose the dielectric object, such as polytetrafluorethylene (PTFE), Nylon, and Lien, which is easy to attract electrons and widely utilized in wearable applications, to develop the STEG with the conductive fabric. When a dielectric object contacts the conductive fabric, the surface of the dielectric object and fabric electrode compose a friction pair. Owing to the difference in electron-attracting abilities between the two surfaces, charges will be transferred, thus making the supercapacitor positively charged through a rectifier circuit. Subsequently, when the

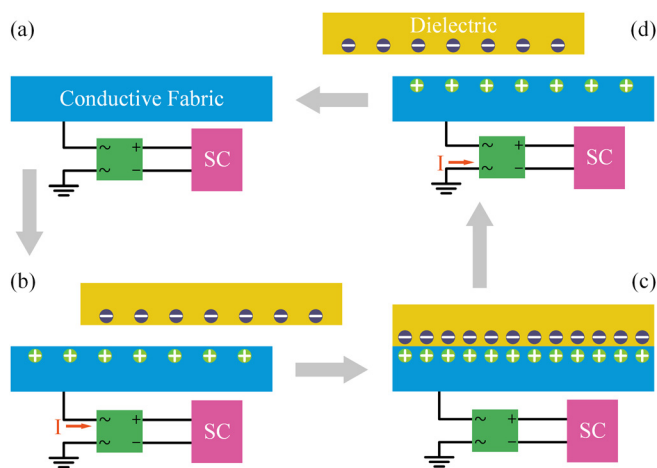


FIG. 2. Working mechanism and electrical distribution of the SCPC with four states. (a) The original state, (b) contacting state with positive charging, (c) completed contact state, and (d) separating state with reverse charging.

charged active object separates from the fabric electrode, a potential difference forms between the conductive fabric and the grounded reference electrode. Charges will transfer to reach an electrostatic equilibrium state, which brings in the supercapacitor reversely charged and accomplish one charging cycle.

In order to evaluate the electrochemical performance of the assembled flexible supercapacitor, the device is overall tested through cyclic voltammetry (CV), galvanostatic charge-discharge (GCD), Nyquist plots, Ragone plots, and cycling stability using an electrochemical workstation. First, the device is analyzed by CV curves with the scan rates ranging from 10 mV/s to 200 mV/s at a stable potential window [Fig. 3(a)]. Definitely, the CV curves retain their quasi-rectangular shape and are approximately symmetrical about the zero-current line, thus indicating the ideal double-layer electrochemical behavior.

Then, the GCD test is also carried out as shown in Fig. 3(b), where the typical GCD curves are performed, the charging-discharging currents of which are from 2 mA to 10 mA. Evidently, GCD curves reveal that all of the charging curves are symmetrical with their corresponding discharging counterparts. Besides, the areal capacitance is achieved according to the (1) with the CV curves of the supercapacitor

$$C_A = \frac{Q}{A \times \Delta V} = \frac{1}{k \times A \times \Delta V} \int_{V_1}^{V_2} I(V) dV, \quad (1)$$

where C_A is the areal capacitance, $I(V)$ is the discharge current function, k is the scan rate, and A is the area of the device. ΔV is the potential window during the discharge process, where V_1 and V_2 are the maximum and minimum voltage values, respectively. With the scan rate of the device at the 10 mV/s, it could achieve the maximum areal capacitance of 16.76 mF/cm², which decreases slightly with the increase in the scan rates [Fig. 3(c)].

In addition, the impedance behavior as shown in Fig. 3(d) further confirms the frequency response of the supercapacitor, demonstrating the satisfactory charge transfer resistance of the device. Both the energy and power density of the device at the initial state could be further achieved by the following equations:

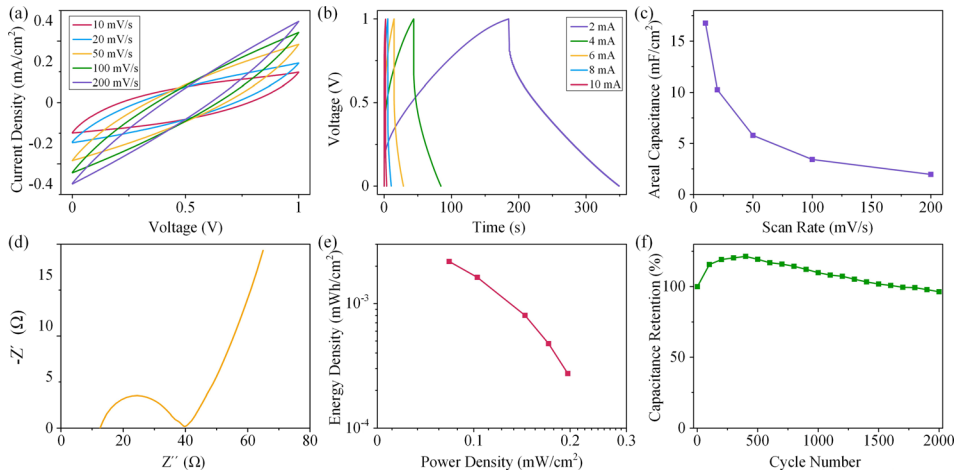


FIG. 3. Electrochemical behavior of the supercapacitor. (a) CV curves, (b) GCD curves, (c) areal capacitance, (d) Nyquist plots, (e) Ragone plots, and (f) cycling stability of the device.

$$E = \frac{1}{2 \times 3600} C_V (\Delta V)^2, \quad (2)$$

$$P = \frac{E}{\Delta t} \times 3600, \quad (3)$$

where Δt is the discharging time, E is the energy density, and P is the power density. The highest energy density is 0.0022 mW h/cm^2 at the scan rate of 10 mV/s , and at the same time, the highest power density is 0.197 mW/cm^2 at the scan rate of 200 mV/s , respectively. Definitely, both of them vary slightly with the increase in scan rates as shown in Fig. 3(e). As for the cycling stability, the capacitance retention of the supercapacitor maintains more than 96% of the initial capacitance after 2000 cycles [Fig. 3(f)]. Therefore, such a flexible supercapacitor shows stable and excellent electrochemical performance, which could satisfy the needs of a self-charging power unit.

Afterwards, Fig. 4 shows the output performance of the STEG under periodic impacts with different frequencies via a vibration system. Considering the application of the wearable system, PTFE is tested because they are widely used as sports clothes. The STEG works well over a frequency of

$1 \text{ Hz} - 7 \text{ Hz}$, where continuous periodic outputs are generated. Both the voltage and current waveforms are quite uniform and fairly symmetrical, and the outputs become larger with the increasing frequency [Figs. 4(a) and 4(b)]. More importantly, the STEG is used to charge a $1 \mu\text{F}$ capacitor to test the capability of the power output. With a rectifier circuit to convert the alternating current into direct current, the voltage of the capacitor reaches $\sim 5 \text{ V}$ after 4 min vibration and charging process as shown in Fig. 4(c). The device also obtains good stability for 10 000 cycles [Fig. 4(d)], retaining almost the same output and capable of satisfying the stable charging process. Notably, with the best-matched load resistance of $300 \text{ M}\Omega$, the peak output power density reaches $12.1 \mu\text{W/cm}^2$ as shown in Fig. S4. Such a remarkable output proves that SCPC is a promising candidate for harvesting mechanical energy efficiently and charging energy storage device effectively.

As for the self-charging display, STEG is utilized to charge the supercapacitor via a switch circuit as shown in Fig. 5(a). While working in the energy-harvesting mode (S_1 on and S_2 off), the STEG could convert the mechanical energy into electrical energy stored in the supercapacitor

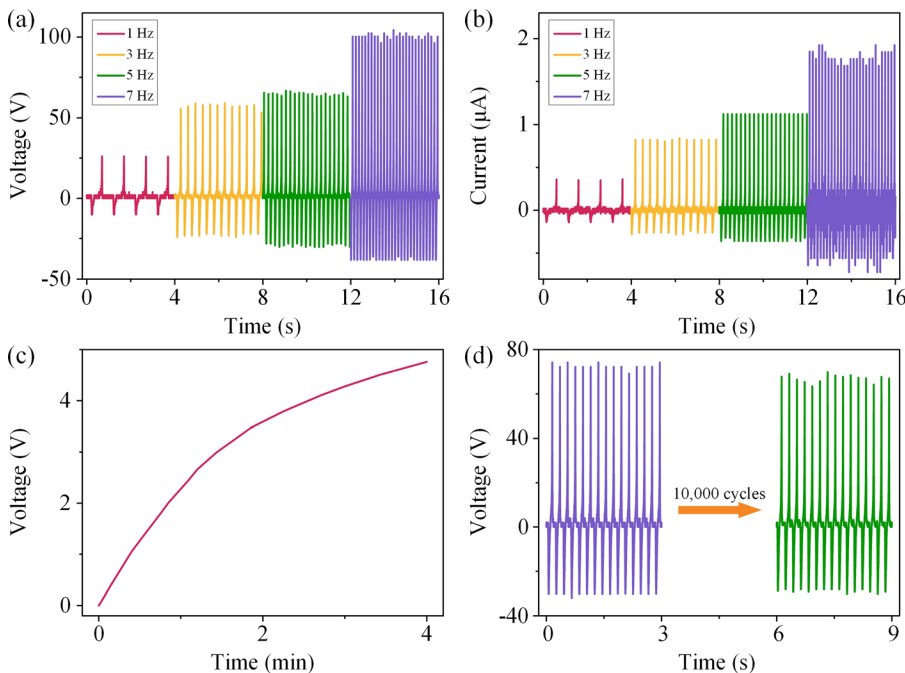


FIG. 4. Output characterization of the STEG. (a) The output voltage and (b) current waveforms at various frequencies. (c) The charging curve of a $1 \mu\text{F}$ capacitor and (d) output stability after 10 000 cycles.

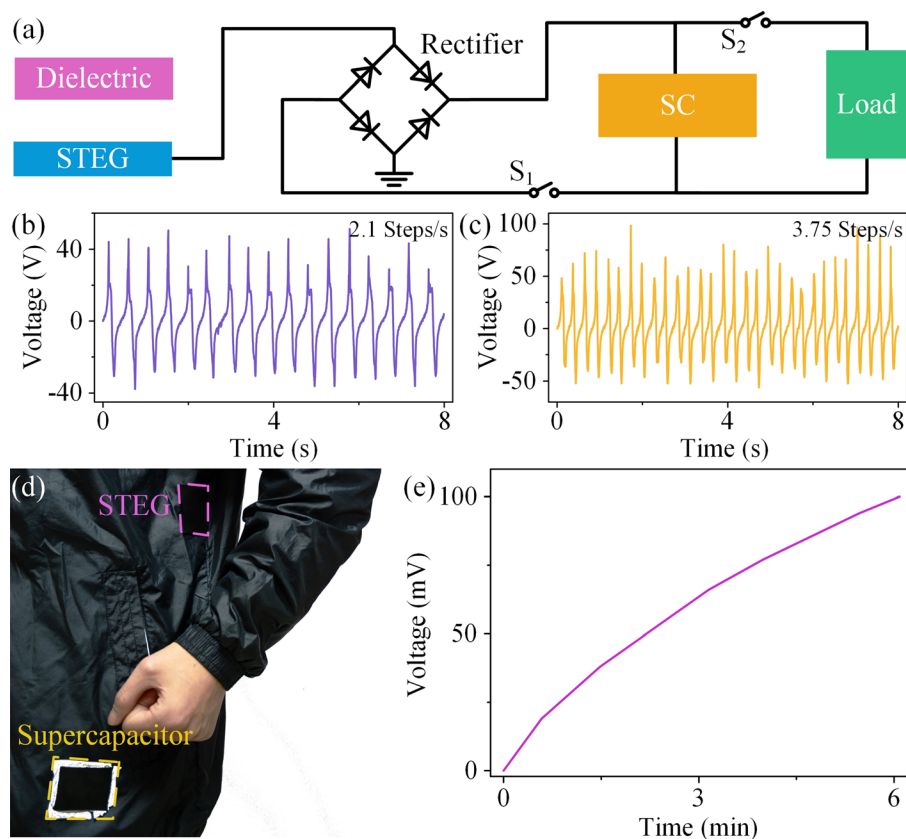


FIG. 5. Self-charging performance of SCPC. (a) Circuit diagram of the SCPC with energy storage and supply mode. Output voltage of the STEG during the (b) walking and (c) running human motions. (d) Wearable display of SCPC attached among the cloth surface. (e) Initial charging curves of the SCPC during the running motions.

component. As shown in Figs. 5(b) and 5(c), the STEG exerts about periodic 2.1 Hz and 3.75 Hz output signals under the normal walking and running motions, respectively, which corresponds to the frequency of the step movement. The prototype of the SCPC in the cloth is demonstrated in Fig. 5(d). Specifically, when woven among the body side cloth, the STEG will contact the arm every step during the human motion and harvest the mechanical energy effectively. Under the normal running motion, the supercapacitor (0.5 cm^2) could be gradually charged to 100 mV within 6 min [Fig. 5(e)], which brings significant advancement for self-charging wearable technology. After sufficient amounts of charges have been stored, the SCPC could transform into the energy supply mode (S_1 off and S_2 on). Three SCPCs connected in series could drive a calculator to perform a series of calculations. The calculator could stably work the complex arithmetic for more than 7 min (Fig. S5), which demonstrates that SCPC could drive low-power electronic system sustainably.

In summary, we propose a self-charging power cloth with a general CNT/cotton fabric electrode. On the one hand, attached to the body side, the wearable STEG could stably scavenge human mechanical energy during the walking or running motions. On the other hand, the solid-state supercapacitor shows excellent performance and mechanical strength, which enables it as an ideal flexible energy storage device. During human motions, the SCPC can be utilized to simultaneously harvest and convert the mechanical energy into electrochemical energy. Therefore, with high integration and wearable compatibility, this SCPC shows promising potential in self-powered wearable devices and smart cloths.

See [supplementary material](#) for the digital image, resistance change with dropping time and washing time of flexible fabric electrode, power output of the STEG, and the calculator driven by SCPC.

This work was supported by National Key R&D Project from Minister of Science and Technology, China (2016YFA0202701), the National Natural Science Foundation of China (Grant No. 61674004, 61176103 and 91323304), and the Beijing Natural Science Foundation of China (Grant No. 4141002).

- ¹H. Chen, Z. Su, Y. Song, X. Cheng, X. Chen, B. Meng, Z. Song, D. Chen, and H. Zhang, *Adv. Funct. Mater.* **27**, 1604434 (2017).
- ²J. Han, B. Kim, J. Li, and M. Meyyappan, *Appl. Phys. Lett.* **102**, 051903 (2013).
- ³S. Li, Q. Zhong, J. Zhong, X. Cheng, B. Wang, B. Hu, and J. Zhou, *ACS Appl. Mater. Interfaces* **7**, 14912 (2015).
- ⁴Y. Song, X. Chen, J. Zhang, X. Cheng, and H. Zhang, *J. Microelectromech. Syst.* **30** (2017).
- ⁵Z. Wen, M. Yeh, H. Guo, J. Wang, Y. Zi, W. Xu, J. Deng, L. Zhu, X. Wang, and C. Hu, *Sci. Adv.* **2**, e1600097 (2016).
- ⁶X. Pu, L. Li, H. Song, C. Du, Z. Zhao, C. Jiang, G. Cao, W. Hu, and Z. L. Wang, *Adv. Mater.* **27**, 2472 (2015).
- ⁷J. Wang, X. Li, Y. Zi, S. Wang, Z. Li, L. Zheng, F. Yi, S. Li, and Z. Wang, *Adv. Mater.* **27**, 4830 (2015).
- ⁸W. Liu, Z. Chen, G. Zhou, Y. Sun, H. R. Lee, C. Liu, H. Yao, Z. Bao, and Y. Cui, *Adv. Mater.* **28**, 3578 (2016).
- ⁹X. Lu, M. Yu, G. Wang, Y. Tong, and Y. Li, *Energy Environ. Sci.* **7**, 2160 (2014).
- ¹⁰L. Zhang and X. Zhao, *Chem. Soc. Rev.* **38**, 2520 (2009).
- ¹¹P. Du, X. Hu, C. Yi, H. C. Liu, P. Liu, H. L. Zhang, and X. Gong, *Adv. Funct. Mater.* **25**, 2420 (2015).
- ¹²Y. Zi, S. Niu, J. Wang, Z. Wen, W. Tang, and Z. L. Wang, *Nat. Commun.* **6**, 8376 (2015).
- ¹³X. Cheng, Y. Song, M. Han, B. Meng, Z. Su, L. Miao, and H. Zhang, *Sens. Actuators, A* **247**, 206 (2016).

- ¹⁴B. Meng, X. Cheng, X. Zhang, M. Han, W. Liu, and H. Zhang, *Appl. Phys. Lett.* **104**, 103904 (2014).
- ¹⁵Y. Song, X. Cheng, H. Chen, J. Huang, X. Chen, M. Han, Z. Su, B. Meng, Z. Song, and H. Zhang, *J. Mater. Chem. A* **4**, 14298 (2016).
- ¹⁶G. Zhu, W. Q. Yang, T. Zhang, Q. Jing, J. Chen, Y. S. Zhou, P. Bai, and Z. L. Wang, *Nano Lett.* **14**, 3208 (2014).
- ¹⁷X. Zhang, J. Brugger, and B. Kim, *Nano Energy* **20**, 37 (2016).
- ¹⁸J. Wang, Z. Wen, Y. Zi, P. Zhou, J. Lin, H. Guo, Y. Xu, and Z. L. Wang, *Adv. Funct. Mater.* **26**, 1070 (2015).
- ¹⁹X. Zhang, M. Su, J. Brugger, and B. Kim, *Nano Energy* **33**, 393 (2017).
- ²⁰M. Shi, J. Zhang, M. Han, Y. Song, Z. Su, and H. Zhang, in *Proceedings of the 29th International Conference on Micro Electro Mechanical Systems (MEMS)*, Shanghai (2016), p. 1228.